Engineering Science and Technology, an International Journal 21 (2018) 564–573

HOSTED BY

Contents lists available at ScienceDirect

Engineering Science and Technology, an International Journal

journal homepage: www.elsevier.com/locate/jestch

Full Length Article

Geographic information system and weather based dynamic line rating for generation scheduling

Ram Jethmalani C. Hemparuva [a,*], Sishaj P. Simon [b], Sundareswaran Kinattingal [b], Narayana Prasad Padhy [c]

[a] Department of EEE, National Institute of Technology, Puducherry, India
[b] Department of EEE, National Institute of Technology, Tiruchirappalli, India
[c] Department of Electrical Engineering, Indian Institute of Technology, Roorkee, India

ARTICLE INFO

Article history:
Received 9 November 2017
Revised 24 April 2018
Accepted 18 May 2018
Available online 19 June 2018

Keywords:
Geographic information system
Dynamic line rating
IEEE 738 guidelines
Binary real coded particle swarm optimization
Security constrained unit commitment
AC-optimal power flow

ABSTRACT

Transmission line ratings influence the economic and security aspects of power system operation, generation and planning. The use of geographical information systems in power system generation and planning activities is gaining importance. This paper proposes a geographical information system and weather based dynamic line rating (GISWDLR) and investigates its effectiveness in a security constrained unit commitment problem (SCUCP). Here, the dynamic line ratings (DLRs) of conductors at different locations along the transmission line are calculated using the geographic parameters and weather parameters. Thereafter, the minimum value of DLRs at all indentified locations of the transmission line is taken as DLR of the transmission line. Here, binary real coded particle swarm optimization (BRPSO) is employed to solve the SCUCP. The proposed method is validated using the benchmark IEEE 30 bus system. Here, results obtained using the proposed GISWDLR, static line rating (SLR) and conventional UCP are compared. Also, the effectiveness of BRPSO is validated by comparing it with the conventional enhanced priority list based method.

© 2018 Karabuk University. Publishing services by Elsevier B.V. This is an open access article under the CC BY-NC-ND license (http://creativecommons.org/licenses/by-nc-nd/4.0/).

1. Introduction

In a restructured power system, the independent system operator (ISO) dispatch centre prepares the schedule for the next day by solving scheduling problems such as security constrained unit commitment problem (SCUCP) or profit based unit commitment problem (PBUCP). In restructured markets, including the PJM interconnection, the New York market, and the U.K. Power Pool, the ISO plans the day-ahead schedule using security-constrained unit commitment. Here, the ISO collects detailed information on each generating unit including characteristics such as start-up costs, minimum up time and minimum down time, minimum and maximum unit outputs, and bids representing incremental heat rate from the generation companies (GENCOs). The ISO also obtains information from transmission companies (TRANSCOs) on transmission line capability and availability. Then, the ISO uses the SCUC model to determine the optimal allocation of generation resources [1]. The power transfer limit of transmission lines is an important constraint for solving the power system scheduling problem (PSSPs). This constraint plays an essential role in the secure and economic management of the power system [2,3]. The available transmission line capacity is calculated using the value of maximum power transfer limit. Therefore, considering the above process, the objective of this article is to improve the solution quality of SCUCP, in which dynamic transmission line ratings are considered.

A geographic information system (GIS) is designed to work with data referenced by spatial or geographic coordinates [4]. The smart grid aims to integrate information systems into existing power systems [5]. GIS is used as a tool to enable effective power system functions such as network planning, outage response, asset management, by the power utilities [6,7]. GIS along with the weather parameters are used in this article to calculate transmission line ratings. These transmission line ratings are used to solve the PSSPs. Ampacity of a transmission line is the maximum current it can carry without either reducing the tensile strength or exceeding the maximum permitted sag [8]. This current limit is translated into power transmission limit. Traditionally, thermal ratings are calculated seasonally assuming given conservative weather condi-

* Corresponding author at: Department of EEE, National Institute of Technology, Puducherry, India.
E-mail address: malanisuryakumaran@gmail.com (R.J.C. Hemparuva).
Peer review under responsibility of Karabuk University.

https://doi.org/10.1016/j.jestch.2018.05.011
2215-0986/© 2018 Karabuk University. Publishing services by Elsevier B.V.
This is an open access article under the CC BY-NC-ND license (http://creativecommons.org/licenses/by-nc-nd/4.0/).

Nomenclature

Parameters, functions and variables

B	Susceptance of transmission line
$CLOL$	Cumulative loss of load
C_1	Cognitive scaling factor
C_2	Social scaling factor
FC	Fuel cost
$FitB$	Fitness of binary string.
$FitR$	Fitness of a real string used in solving OPF.
G	Conductance of transmission line
Gb	Global best position
H_e	Conductor elevation from sea level
I_i^t	ON/OFF status of generating station 'i' and schedule interval 't'
K	Spinning reserve requirement
L_t	Latitude of location
L_n	Longitude of location
$MOVI$	Minimum ON/OFF violation index
N	Day number in a year
N_{bp}	Number of binary coded particles
N_{rp}	Number of real coded particles
nc	Number of shunt capacitor banks
ng	Number of generators
nl	Number of transmission lines
OC	Operational cost
Pb	Particle best position
PT_{Loc}^{max}	Maximum power transfer limit at a location
PT_{Line}^{max}	Maximum power transfer limit of a transmission line
$P_{i,t}$	Power generated by generator 'i' in interval 't'
$P_{Di,t}$	Power demand at bus 'i' in interval 't'
PRM	Real power mismatch in percentage
PQM	Reactive power mismatch in percentage
q_c	Heat dissipated by a conductor through convection
QI	Reactive power injection
QD	Reactive power demand
q_s	Solar heat gain
$QG_{i,t}$	Reactive power generated by generator 'i' in interval 't'
$QGLV$	Reactive power limit violation index
QM	Reactive power balance mismatch
RM	Real power balance mismatch
SD_i^t	Shut down cost of generator 'i' in interval 't'
SU_i^t	Startup cost of generator 'i' in interval 't'
SI	Severity index
T	Number of schedule intervals
T_a	Ambient temperature
$T_{i,t}^{ON}$	Minimum up-time of generator 'i'
$T_{i,t}^{OFF}$	Maximum up-time of generator 'i'
Rd_i	Ramp up limit of generator 'i'
Rp_i	Ramp down limit of generator 'i'
$V_{i,t}$	Magnitude of voltage at bus 'i' in interval 't'
Vl	Velocity of best particle
w_d	Wind direction
w_s	Wind speed
X_I	Binary PSO particle representing ON/OFF status
$X_{i,t}^{ON}$	'ON' duration of generator 'i' till interval 't'
$X_{i,t}^{OFF}$	'OFF' duration of generator 'i' till interval 't'
z_l	Azimuth angle of transmission line
ρ_f	Density of air surrounding the conductor
W	Inertia

Parameters, functions and variables

i	Generator index
I	Particle index
k	Iteration count
t	Time interval index

tions. These static line ratings (SLR) mostly lead to conservative operational limits. Also, SLRs are over estimated at extreme weather conditions as they ignore the impact of weather on the line capacity [9]. DLR is also a useful approach to provide temporary additional transmission capacity while ensuring the power system security with higher loading of transmission lines [3].

If most of the economic units are located in one region of the system, it becomes more difficult to satisfy network constraints throughout the system. As the network becomes more congested, the system operator should incorporate the network flow constraints in the PSSP to minimize the violation and the related costs of the normal operation of the system [10]. The maximum power transferred (PT^{max}) by a conductor depends on temperature of the transmission line. The temperature of the transmission line is influenced by the following factors [11]:

1. Ambient weather conditions such as the wind speed, wind direction, solar radiation and precipitation.
2. The geographic orientation of conductor such as the line direction and line height.
3. Specification of the conductor including conductor size, resistance, sag and the type of conductor surface.
4. Current flowing through the conductor.

The models to obtain temperature and current of a transmission line are discussed in IEEE 738 guidelines [11]. Methods to determine the power transmission limit is categorised as follows [12,13]:

1. Weather forecast based systems
2. Temperature measurement based systems
3. Sag monitoring based systems

In [14], a DLR forecast system using probabilistic approach is proposed. Here, the historical data of weather and power transmitted are used. In [15], DLR values are obtained using weather parameters and conductor temperature monitoring system. In [16], sag of transmission lines are measured using tension monitoring systems. Here, tension monitors are installed between dead-end insulators and the dead-end structure of the transmission lines. The tension measured using the monitors are used to calculate sag of the transmission line, which is used to calculate the transmission line rating of the transmission line. In [17], DLR of transmission lines are calculated using temperature sensors placed on the transmission lines. In [18], expert systems are used to predict DLR of transmission lines. In [19], a linear model to calculate DLR based on meteorological data is presented. In [20], weather prediction models are used along with machine learning algorithms are used to predict DLR of transmission lines. In [21], major considerations in selection of DLR various DLR systems are discussed. In [22] the increased use of weather forecast on predicting DLR is discussed. In [23], different line rating forecasting methods are compared. The commercially available DLR monitoring systems along with short description on the operation principle is given in Table 1.

In [9], the effect of DLR on economic dispatch of generators with wind power integration is investigated. Also, the use of DLR in

Table 1
Real time DLR monitoring systems.

DLR system	Description
Power Donut	A donut shaped device installed on the transmission line measures the temperature and inclination of line. These measurements are used to obtain the sag of the conductor and consequently the DLR
CAT I	Mechanical tensions at extremities are measured to calculate sag of the transmission line
Ampacimon sag calculator	Sag of the transmission line is calculated using vibration data.
Fiber optic cable method	A fibre optic cable is wrapped over the conductor. The fibre optic device provides accurate measurement of temperature and tension over the whole length of line. These measurements are used to calculate sag and thereby the DLR.
Lasertech.	The distance between the transmission line and conductor is measured using a laser based system. This distance is the sag and therefore, the DLR is calculated.
Sag measurement using camera.	The sag is calculated by visual verification using a camera.
Sag measurement using GPS.	Sag in transmission line is measured by using the GPS information which can bring out the coordinates and height of the conductor above ground level.
Net radiation sensor.	The point measurement of solar input is measured. This solar input is used to calculate the line tension and clearance which influences DLR.
Sag stop watch.	The return time of a reflected wave is a function of length and size of the conductor. The DLR of transmission line is calculated using the return time, which is a function of conductor sag.
Real time SONAR instrument.	Sonar technology measures the time taken by a 20 kHz sound pulse to travel from sonar head fixed on the conductor to ground and return back to the sonar head. This time is used to calculate the sag.

solving unit commitment problem with intermittent wind power is investigated in [24]. Integration of DLR in real time optimal dispatch is carried out in [25]. Use of DLR in solving a security constrained economic dispatch using heat balance equations and benders decomposition is investigated in [2]. Though there are different commercial dynamic line rating (DLR) monitoring equipments, they do not seem to be extensively used or established technology yet [8]. In this context, this paper proposes a method to use geographic information system and weather based dynamic line rating (GISWDLR).

2. Problem formulation

Conventionally, the schedule of generators connected to a power system is obtained by solving power system scheduling problems such as unit commitment problem and economic dispatch sub-problem [26–29]. In this article, the generator schedules are obtained by solving a security constrained economic dispatch problem. Here, the hourly power dispatch is obtained by solving an AC-optimal power flow (AC-OPF) problem with security constraints. These security constraints are limited by the transmission line ratings.

2.1. Dynamic rating of transmission lines [11]

The amount of power transmitted by a transmission line is limited by the maximum temperature the line can withstand. Temperature of a transmission line is a function of factors such as the conductor dimensions, ambient weather conditions prevailing around the transmission line, the geographic location and orientation of the transmission line. Here, these parameters govern the heat balance equation and in turn influence the temperature rise of a transmission line. The heat balance equation relates the amount of heat entering into the transmission line, heat dissipated from the transmission line and the heat stored. The maximum apparent power transferred by a conductor (PT^{max}) at an instant is calculated using (1). Here, the heat balance equation of a conductor comprises of three components namely, the convective heat loss by the conductor (q_c), radiative heat loss by the conductor (q_r), and the solar heat gained by the conductor (q_s). These heat components are functions of geographic and weather variables. The reader may refer IEEE 738 standards for detailed equations of these components.

$$PT^{max} = V_R\sqrt{\frac{q_c + q_r - q_s}{R_T}} \tag{1}$$

where V_R and R_T are the base voltage of the system and resistance of the conductor, respectively.

2.2. Generation scheduling and SCUCP

The objective of a unit commitment problem (UCP) is to find an optimal schedule to commit the generating units, which minimizes the operation cost (2) for meeting the forecasted system load while satisfying the power balance constraint (25), unit constraints (26), minimum ON/OFF constraints (27), and spinning reserve constraints (28) [30]. The schedule obtained by solving a UCP may be infeasible if the network security constraints are violated. Therefore, security constrained UCP is an extension of UCP in which the network security constraints (29) are also considered along with other constraints.

$$\text{Minimize OC} = \sum_{t=1}^{T}\sum_{i=1}^{ng} f_i(P_{i,t})I_{i,t} + SU_i^t I_i^t(1 - I_{i,t-1}) + SD_i^t(1 - I_{i,t}) \tag{2.a}$$

$$f_i(P_{i,t}) = a_i + b_i P_{i,t} + c_i P_{i,t}^2 + |e_i \sin(f_i(P_{min,i} - P_{i,t}))| \tag{2.b}$$

Subject to:

$$P_{m,t} - P_{Dm,t} = V_{m,t}\sum_{n=1}^{nb}\{|V_{n,t}|(G_{mn}\cos\theta_{mn} + B_{mn}\sin\theta_{mn})\} \quad m \in \{1,2\ldots,nb\} \tag{3.a}$$

$$QG_{m,t} - QD_{m,t} = V_{m,t}\sum_{n=1}^{nb}\{|V_{n,t}|(G_{mn}\sin\theta_{mn} + B_{mn}\cos\theta_{mn})\} \quad m \in \{1,2\ldots,nb\} \tag{3.b}$$

$$P_{min,i} \leqslant P_i \leqslant P_{max,i} \text{ for } i = 1,2,\ldots ng \tag{4.a}$$

$$QG_{min,i} \leqslant QG_{i,t} \leqslant QG_{max,i} \text{ for } i = 1,2,\ldots ng \tag{4.b}$$

$$X_{i,t}^{ON} \geqslant T_{i,t}^{ON} \rightarrow I_{i,t-1} - I_{i,t} = 1 \tag{5.a}$$

$$X_{i,t}^{OFF} \geqslant T_{i,t}^{OFF} \rightarrow I_{i,t} - I_{i,t-1} = 1 \tag{5.b}$$

$$\sum_{i=1}^{N} P_{max,i}I_{i,t} \geqslant PD_t K \tag{6}$$

$$V_i^{min} \leqslant V_{i,t} \leqslant V_i^{min} \tag{7.a}$$

$$|PT_{i,t}| \leqslant PT_i^{max} \text{for } i = 1,2,\ldots,nl \tag{7.b}$$

In a conventional SCUCP, the transmission line ratings are calculated by considering system variables (weather and geographic) under worst case scenario. However, in DLR based SCUCP, the transmission line ratings for each interval is calculated based on

the forecasted value of these independent variables. Since the transmission line ratings vary at each time interval, the solution space available for the scheduling algorithm keeps on varying for each schedule interval. Therefore, the schedule obtained by solving the scheduling problem will also vary and the operating cost of power system will also alter.

3. Proposed methodology

3.1. Weather based dynamic line rating

The maximum power transferred by a transmission line will differ from point to point along the transmission line as the weather and geographic location of the transmission line is not constant throughout its length. Therefore, the actual DLR of a transmission line is the minimum value of PT^{max} obtained at all points along the transmission line. The reliability of the obtained DLR is proportional to the number of points considered. It may not be feasible to obtain data for all points along the transmission line. Therefore, in the proposed methodology, line rating of conductor at different locations along the conductor is considered. Here, the geographic and weather parameters at the locations are obtained through GIS and internet based weather forecasts. The procedure to obtain DLR of a transmission line is given below.

1. Obtain the geographical layout of the power system network.
2. Identify the transmission lines in which DLR can be used. The line selection is based on criteria such as location data availability and weather station availability.
3. For each identified transmission lines, obtain the route from the starting bus 'I' to the ending bus 'J' and locate notable cities/villages in the route.
4. Locate weather stations nearest to each of the noted locations.
5. Obtain geographic parameters of each location, such as latitude (L_t), height of the location from sea level (H_e), and transmission line direction (z_l) using the geographic information system.
6. Obtain weather parameters such as ambient temperature (T_a), wind speed (w_s), and wind direction (w_d) at the identified locations for the entire schedule horizon using weather monitoring and forecasting system.
7. Obtain the maximum apparent power transferred by conductor in the selected location (PT^{max}) using Eq. (1). Here, the input variables are the geographic and weather variables.
8. Obtain DLR of the transmission line by choosing the minimum value of (PT^{max}) obtained for different locations in the transmission lines using Eq. (2).

$$PT^{max}_{Line} = \min\{PT^{max}_{Loc1}, PT^{max}_{Loc2}, \ldots PT^{max}_{LocN}\} \tag{2}$$

3.2. BRPSO for SCUCP

In SCUCP, the binary numbers 1 and 0 are used to represent the unit ON/OFF status. Though there are various non-conventional heuristic algorithms, particle swarm optimization (PSO) is chosen as it is seen as a promising optimization tool from the literature [31–33]. PSO is a real coded algorithm which needs modifications to adapt the binary representations of SCUCP problem. In binary PSO, the variables are interpreted in terms of changes in probabilities. Here, the position of particle takes either 0 or 1 [34]. The steps involved in solving SCUCP using binary PSO and AC-OPF for each hourly interval using real coded PSO are given in Sections 3.2.1 and 3.2.2, respectively.

3.2.1. Binary coded PSO

1. Randomly generate N_{bp} number of initial particles. The representation of a particle X_I is shown below. Here, $I_{t,i}$ is the ON/OFF status of i^{th} generator at t^{th} schedule interval.

$$X_I = \begin{bmatrix} I_{1,1}I_{1,2}\ldots I_{1,i}\ldots I_{1,ng}I_{2,1}I_{2,2}\ldots I_{2,i}\ldots I_{2,ng\ldots} \\ \ldots I_{t,1}I_{t,2}\ldots I_{t,i}\ldots I_{t,ng}\ldots I_{T,1}I_{T,2}\ldots I_{T,i}\ldots I_{T,ng} \end{bmatrix}$$

2. Repair the particles to satisfy minimum ON/OFF constraints (5) and spinning reserve constraints (6) [32].
3. Evaluate the fitness of each particle using (9). Here, the fitness of each particle is formulated based on the operating cost (OC), cumulative loss of load (CLOL) and minimum ON/OFF violation index (MOVI). The operating cost of a binary string is obtained by solving AC-OPF for each of the schedule interval using real coded PSO.MOVI and CLOL are defined in (10) and (11), respectively.

$$FitB = \frac{1}{1 + OC(1 + CLOL)(1 + MOVI)} \tag{9}$$

$$MOVI = \sum_{t=1}^{T}\sum_{i=1}^{ng} \begin{matrix} min\left\{(T^{ON}_{i,t} - X^{ON}_{i,t}), 0\right\} \\ +min\left\{(T^{OFF}_{i,t} - X^{OFF}_{i,t}), 0\right\} \end{matrix} \tag{10}$$

$$CLOL = \sum_{t=1}^{T} \begin{Bmatrix} max\{(\{\sum_{i=i}^{ng} I_{i,t}P_{maxi,t}\} - KP_{Di,t}), 0\} \\ max\{(KP_{Di,t} - \left\{\sum_{i=i}^{ng} I_{i,t}P_{min,t}\right\}), 0\} \end{Bmatrix} \tag{11}$$

4. Update the fitness and position of local best particles and the global best particle [33].
5. For each of the particles, update velocity using Eq. (12).

$$Vl_I = WVl_I + C_1R_1(Pb_I - X_I) + C_2R_2(Gb - X_I) \tag{12}$$

6. Update the binary position representing ON/OFF status of generators. If the absolute velocity of a particle corresponding to a generator is larger than a preset threshold limit, then it's ON/OFF status is altered as in (13).

$$I_{t,i} = I_{t,i}\prime \tag{13}$$

7. If the iteration count reaches its maximum, then terminate the search. Else, go to step 2.

3.2.2. Real coded PSO

1. Randomly generate N_{rp} number of initial particles. The representation of a particle Y_I is shown below.

$$Y_I = \begin{bmatrix} P_{G1}P_{G2}\ldots P_{Gng}|V|_1|V|_2\ldots|V|_{ng} \\ \delta_1\delta_2\ldots\delta_{nb}QI_1QI_2\ldots QI_{nc} \end{bmatrix}$$

2. Evaluate each particle
   a. For each particle, calculate the parameters such as fuel cost (FC), real power balance mismatch (RM), reactive power balance mismatch (QM), and reactive power generated by generators [35].
   b. Calculate the severity index of each of the particles using the calculated DLR value as in (14).

$$SI = \sum_{i=1}^{nl}\left(\frac{PT_{Linet,i}}{PT^{max}_{Linet,i}}\right)^2 \tag{14}$$

c. Calculate the fitness of each of the particles based on the fuel cost (FC) and penalties for the particles that violate constraints.

$$FitR = \left(\frac{1}{(1-PFC)+(1-PRM) \\ +(1-PQM)+(1-PQGLV)+(1-PSI)} \right) \tag{15}$$

where PFC, PRM, PQM, PQL, and PSI are fuzzy tuned percentage deviation of fuel cost (16), real power balance mismatch (17), reactive power balance mismatch (18), reactive power generation limit violation (19), and severity index (20), respectively [36].

$$PFC = \frac{FC - FC_{min}}{FC_{max} - FC_{min}} \tag{16}$$

$$PRM = \frac{RM - RM_{min}}{RM_{max} - RM_{min}} \tag{17}$$

$$PQM = \frac{QM - QM_{min}}{QM_{max} - QM_{min}} \tag{18}$$

$$PQGLV = \frac{QGLV - QGLV_{min}}{QGLV_{max} - QGLV_{min}} \tag{19}$$

$$PSI = \frac{SI - SI_{min}}{SI_{max} - SI_{min}} \tag{20}$$

where QGLV is the reactive power limit violation index expressed as

$$\left. \begin{aligned} QGLV &= \frac{\sum_{i=1}^{ng}(QGV_{maxi}) + \sum_{i=1}^{ng}(QGV_{mini})}{2*ng} \\ QGV_{maxi} &= 1 \rightarrow QG_i > QG_{\max i} \\ QGV_{mini} &= 1 \rightarrow QG_i < QG_{\min i} \end{aligned} \right\} \tag{21}$$

3. Update the local best fitness, global best fitness, local best position, and global best position.
4. Update velocity and position of all particles.
5. If the maximum number of iteration is reached, then terminate the search. Else, go to step 2.

4. Results and discussions

IEEE 30 bus test system is located in Virginia State of USA. The layout of the system is given in Fig. 1 [37]. The geographic data are obtained using Google Earth. Google Earth is a global GIS which is capable of linking the geological information with the smart grid knowledge [38]. The weather parameters for a sample day (27-April-2016) are obtained from American National Climate Data Center and www.wunderground.com. From Fig. 1, it is seen that buses with number 1 to 7 are located at GlenLyn, Claytor, Kumis, Hancock, Flieldale, Renoke and Blaine. However, the locations of other busses are not available. Therefore, DLR is considered for the eleven transmission lines connected to the above mentioned 7 busses.

4.1. Data collection and DLR

Firstly, the geographical coordinates of each location, is obtained using Google Earth. Then, the road route from a bus at a known location to other bus is identified and notable locations along the route are noted down. Thereafter, the location coordinates, height of the location from the sea level (H_e) and transmission line direction (z_l) are also obtained. Once the locations in each route are noted, the weather parameters in each of the locations are obtained from the weather stations nearest to the location and interpolated to match the number of scheduling interval. The notable locations identified along each of the transmission lines considered for calculation of DLR along with the nearest corresponding weather station is given in Table 2. Here, the line number, location name (LN), the corresponding nearby weather stations (WS) and the number of locations considered in the transmission line (N) are given.

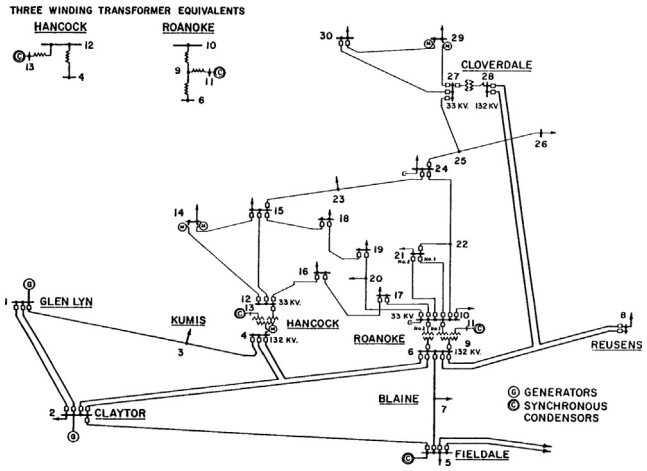

Fig. 1. Layout of IEEE 30 bus system.

Based on the obtained weather parameters and the geographic parameters, the line rating of the transmission lines for each schedule interval. The weather parameters obtained along selected locations in Line 1 for a specific day (27-April-2016) and the calculated DLR are plotted in Fig. 2(a) and (b), respectively. It is seen from Fig. 2 that the DLR of a transmission line is taken as the minimum value among all locations selected along the route. Therefore, a weather condition, which enhances the DLR of a line, may be shadowed due to adverse weather condition in other parts of the line. Also, there is no visible correlation between the weather parameters and the DLR. This is due to the fact that the DLR is influenced by the combined effect of all parameters in all locations of the transmission line.

The line ratings calculated at different locations in Line 1 are plotted against the ambient temperature, wind speed and wind direction in Fig. 3. The statistical parameters of line rating calculated at different locations along Line 1 are plotted against the latitude, height from the sea level and line direction in Fig. 4.

It is observed from Figs. 2–4 that the line rating is influenced by each of the parameters. However, as the DLR is a function of all weather variables and geographic variables, reflection of change in a particular value does not greatly influence DLR. In order to show the influence of a particular variable in the estimation of line ratings, line ratings obtained for different values of the most influencing variables wind speed, wind direction are plotted in Fig. 5. Here, all parameters except wind speed and wind direction are kept constant. Though the influence of any geographic or weather variable is significant in line rating, the DLR plotted in Fig. 2 does not show a visible impact of any particular variable. The reason is due to the combined effect of weather and geographic variables associated with the locations along the line. Hence, the accuracy of DLR estimation increases when geographic information system is used along with weather variables.

Table 2
Location and Weather stations.

Line		Loc1	Loc 2	Loc3	Loc4	Loc5	N
Line1 B1–B2	WS	Narows	Giles county	Staffordsville	UPS Customer Center	Claytor Lake	5
	LN	Glen Lyn	Pearisburg	Cedar Crest Loop	Woodlyn Dublin, VA	Claytor	
Line2 B1–B3	WS	Narows	Pembroke	Newport	Blacksburg	West Virginia Jail	5
	LN	Glen Lyn	Pembroke	New Port Post office	Virginia Tech Montgomery Executive Airport	Kumis	
Line3 B2–B4	WS	Claytor Lake	Lester st Ne	West Virginia Regional Jail	Hancock	–	4
	LN	Claytor Switchyard	Christian burg	Kumis	Hancock	–	
Line4 B3–B4	WS	West Virginia Jail	Hancock	–	–	–	2
	LN	Kumis	Hancock	–	–	–	
Line5 B2–B5	WS	Claytor Lake	Floyd County	Fieldale VA	–	–	3
	LN	Claytor Switchyard	Floyd County	Fieldale	–	–	
Line6 B2–B6	WS	Claytor Lake	Lester st Ne	West Virginia Regional Jail	Hancock	Renoke	5
	LN	Claytor Switchyard	Christian burg	Kumis	Hancock	Renoke	
Line7 B4–B6	WS	Hancock	Renoke	–	–	–	2
	LN	Hancock	Renoke	–	–	–	
Line8 B5–B7	WS	Fieldale VA	Franklin County	–	–	–	2
	LN	Fieldale	Blaine	–	–	–	
Line9 B6–B7	WS	Franklin County	Renoke	–	–	–	2
	LN	Blaine	Renoke	–	–	–	
Line10 B6–B8	WS	Renoke	Bedford city	Reusens	–	–	3
	LN	Renoke	Bedford city	Reusens	–	–	
Line40 B8–B28	WS	Reusens	Forest	Bedford city	Orchards	–	4
	LN	Reusens	Forest	Bedford city	Cloverdale	–	

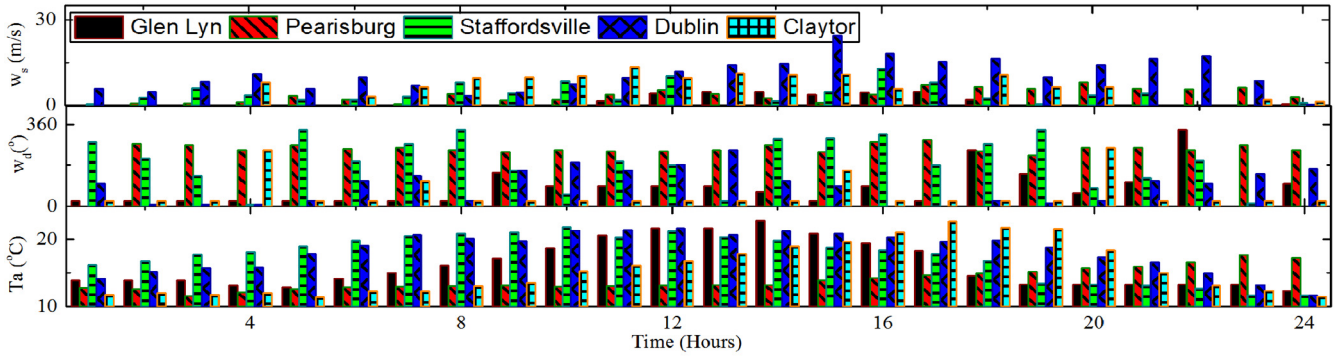

(a)

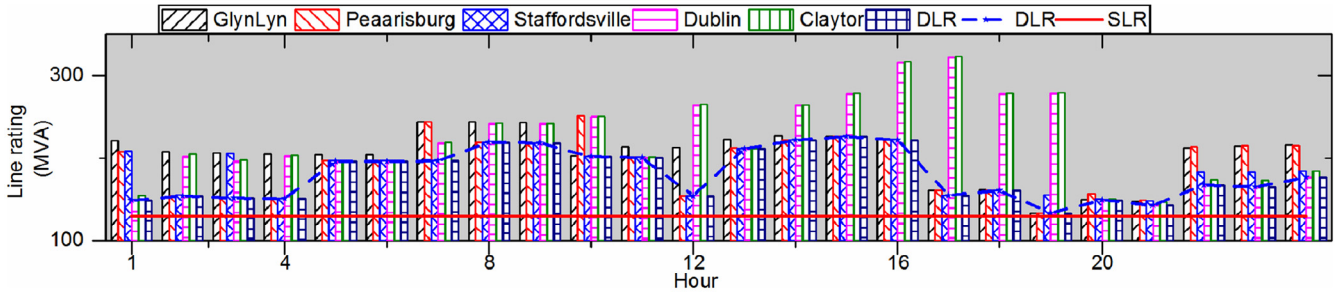

(b)

Fig. 2. (a) Weather parameters at locations along Line 1; (b) DLR and SLR of Line 1.

4.2. Influence of DLR on SCUCP

SCUCP is solved with the proposed DLR using BRPSO and the obtained schedule is given in Table 3. The solution obtained without considering line rating, considering DLR as line rating and SLR as line rating are given in Table 4. It is inferred from Table 3 that the operating cost obtained by solving conventional UCP is lesser than the cost obtained using SCUCP. However, it should be noted that the SI for the schedule obtained by solving conventional UCP is larger. Therefore, the schedule obtained by solving conventional UCP is infeasible due to violation in power transmission limit, which increases the risk associated with the power system.

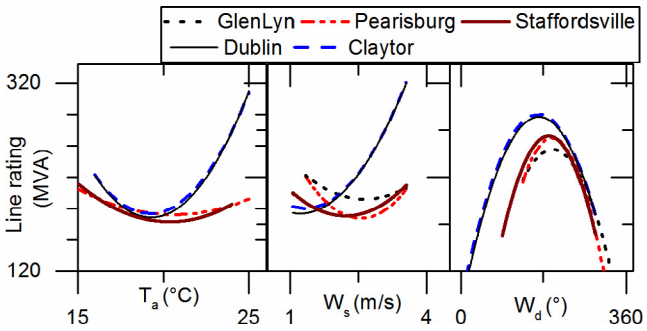

Fig. 3. Influence of weather variables on Line rating.

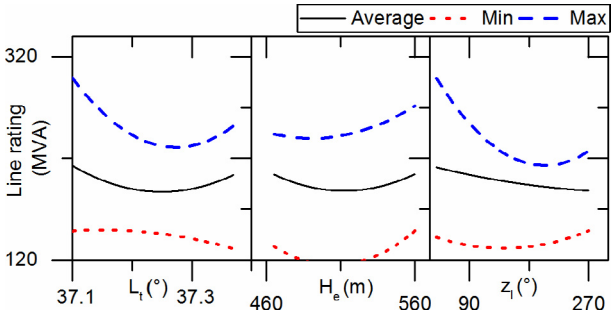

Fig. 4. Influence of Geographic Variables on Line rating.

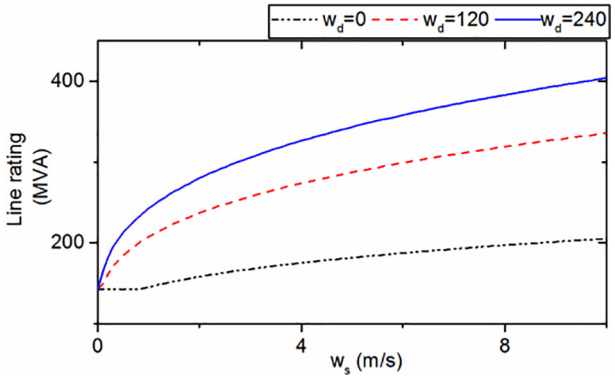

Fig. 5. Decoupled influence of variables on DLR.

The hourly values of power transferred in transmission Line 1 and transmission Line 10 are plotted in Figs. 6 and 7, respectively. Here, the power transferred under all three cases are shown (i.e., No line rating, SLR as line rating, and DLR as line rating).

It is observed that the line ratings for both transmission lines violate their limits when UCP is solved. Though the consideration of SLR reduces the risk associated with the schedule, it constrains the solution space largely and force the search of least operating cost into sub-optimal region. Therefore, the obtained operating cost is larger. The solution of SCUCP with DLR results in a schedule with secure power transmission and less operating cost. It should be noted that, though excess line capacity is available in Line 1, the additional capacity is not utilized for power transmission. In contrast, the additional capacity available in Line 10 is utilized for greater extend. Therefore, consideration of Line 10 for DLR calculation pays more returns compared to consideration of Line 1 for DLR calculations.

4.3. Influence of BRPSO on SCUCP

The proposed BRPSO to solve GISWDLR based SCUCP is compared with enhanced priority list based unit commitment method [39] in Table 5. It is seen that the fuel cost obtained using BRPSO is lesser in comparison to the result of the conventional enhanced priority list method (EPL).

4.4. Influence of forecast error and uncertainty

In order to assess the impact of the forecast uncertainties on the performance of SCUCP-DLR, the operating cost obtained using different values of percentage error in ambient temperature and wind speed forecast are given in Table 6. Here, the percentage error is added to all forecasted weather variable for all time instants. It is observed that the operating cost obtained using SCUCP-DLR is lesser than SCUCP-SLR, even in presence of forecast errors. In order to consider uncertain errors in forecast, percentage error values for different measurements and instants are modified using a random distribution. The percentage error values are obtained using random distribution with zero mean and standard deviations ranging from 0 to 30 percent are tabulated along with the operating cost in Table 7. It is observed that the operating cost increases only if large errors are introduced in the weather forecast. It should be noted that the DLR value obtained with the direct weather measurements station is better than the values given by the online devices [40]. Also, the online devices are more complex and expensive to install and maintain because they imply an installation on the overhead line [40].

4.5. Influence of uncertainty in presence of renewable sources

Additions of renewable power generation sources alter the power flow in transmission lines. Therefore, they alter the operating cost of power system. It should be noted that these sources are variable and adds uncertainty to generation schedule. Therefore, in order to investigate the influence of renewable power generation systems on the proposed model, the SCUCP-DLR is solved assuming a new solar power plant with different level of forecast uncertainty. Here, a hypothetical solar power plant with capacity (P_{SP0} = 50MW) is added at bus 3. The hourly values solar power generations taken for investigation (PV_0) are plotted in Fig. 8. The power generated by the solar power plant is considered as negative demand at bus 3 and the power demand is updated using Eq. (22) [41].

$$P_{D,t} = P_{D,t} - P_{SP,t} \tag{22}$$

The SCUCP is carried out considering the updated power demand [41]. Here, IP0 is considered to be an accurate forecast. In order to investigate the influence of uncertainty in solar forecast, SCUCP is solved considering a forecast with uncertainty (PVF). This forecast is obtained by adding White Gaussian Noise (WGN) to the actual solar power (PV0) [42].The forecasted solar power for each hour is expressed mathematically in Eq. (23), where WGN (μ,σ) is the white Gaussian noise with mean (μ = 0) and standard deviation (σ).

$$PV_F = PV_{F0} + WGN(\mu, \sigma) \tag{23}$$

SCUCP is solved considering the forecasted value of solar power. When this generation schedule is followed, the generators realign to obtain equilibrium in the power balance. This realignment is a result of difference between actual renewable power generations and forecasted value. The realignment of generators can be obtained by automatic generation control or procurement of power in real time market. It should be noted that the cost in real time market and AGC market are larger compared to the cost of

Table 3
Generation Schedule (GISWDLR).

PD	PG1	PG2	PG3	PG4	PG5	PG6	PL	Cost
(MW)								($)
166	50.0	20.0	50.0	35.0	10.0	12.0	11.0	329.8
196	50.0	20.0	50.0	35.0	30.0	12.0	1.0	308.6
229	50.0	54.3	50.0	35.0	10.0	31.2	1.5	285.9
267	50.0	80.0	50.0	35.0	26.1	31.5	5.6	330.0
283.4	121.2	20.0	50.0	35.0	30.0	29.2	2.0	347.9
272	50.0	80.0	50.0	35.0	18.3	40.0	1.3	326.6
246	50.0	80.0	50.0	10.0	30.0	40.0	14.0	336.3
213	75.0	20.0	50.0	35.0	10.0	26.3	3.4	288.6
192	68.6	20.0	15.0	35.0	30.0	40.0	16.6	285.9
161	84.5	20.0	50.0	10.0	10.0	12.0	25.5	328.9
147	50.0	20.4	15.0	10.0	30.0	28.7	7.1	285.9
160	50.0	20.0	50.0	35.0	10.0	0.0	5.0	304.0
170	70.1	20.0	25.0	35.0	17.2	12.0	9.4	285.9
185	58.3	20.0	50.0	35.0	30.0	18.2	26.2	292.1
208	50.0	20.0	50.0	35.0	30.0	24.2	1.2	295.8
232	50.0	20.0	50.0	35.0	30.0	40.0	0.1	285.9
246	119.6	20.0	50.0	35.0	30.0	12.0	20.6	351.6
241	114.4	20.0	50.0	35.0	30.0	12.0	20.4	343.7
236	50.0	41.8	50.0	35.0	30.0	33.2	4.0	285.9
225	50.0	40.0	50.0	35.0	10.1	40.0	0.1	285.9
204	50.0	20.0	50.0	35.0	13.1	40.0	4.1	297.0
182	50.0	20.0	50.0	35.0	30.0	13.3	16.3	307.2
161	50.0	20.7	50.0	35.0	16.9	12.0	24.6	322.8
131	50.0	20.0	50.0	0.0	10.0	20.6	19.6	317.4
Total fuel cost								7429.4
Total operating cost								7457.4

Table 4
Influence of DLR on SCUCP.

	SCUCP- DLR	SCUCP- SLR	UCP
Total fuel cost ($)	7429.4	7543.52	6834.61
Total operating cost ($)	7457.4	7720.52	7094.61
SI	0	0	997.3421

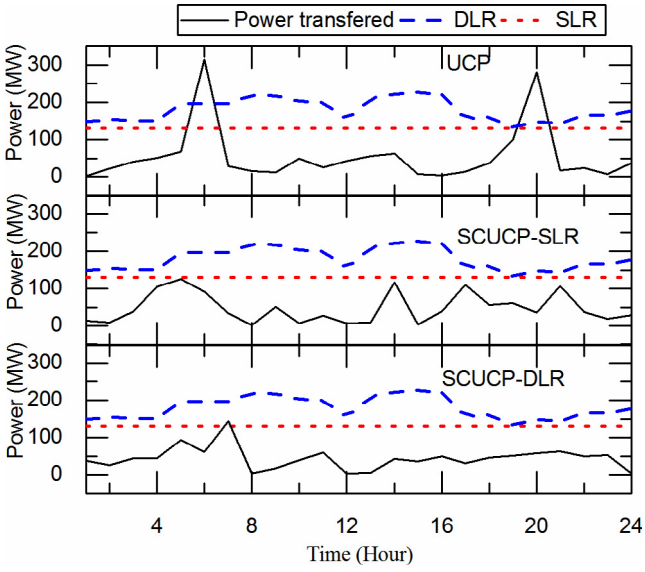

Fig. 6. Power transferred with DLR and SLR in Line 1.

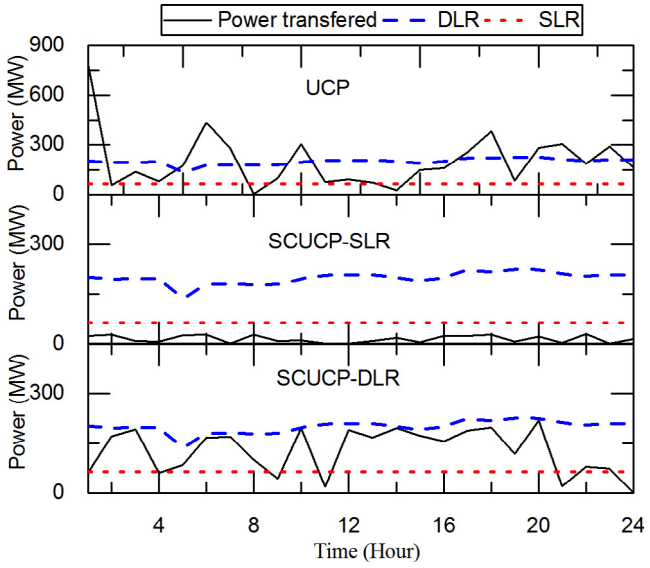

Fig. 7. Power transferred with DLR and SLR in Line 10.

Table 5
Comparison of BRPSO with conventional EPL.

	BRPSO	EPL
Total fuel cost ($)	7429.4	7320.68
Total operating cost ($)	7457.4	7690.68
SI	0	0

generations in day-ahead market The estimated operating cost, rescheduling/regulation cost and actual rescheduled operating cost obtained using the actual and forecasted solar power generation pattern is given in Table 7. Here, the generator number one is assumed to have the AGC regulation contract and hence the mismatch in solar power generation will be supplied by generator1. Here, the rescheduling/regulation cost is taken 1% higher than the fuel cost [43]. It is inferred that the operating cost reduces when solar power plant is considered. The presence of uncertainty in solar power forecast increases the operating cost because of frequent triggering of AGC units or real-time rescheduling.

Table 6
Influence of forecast error on SCUCP-DLR.

Uniform Error		Uncertain Error	
Percentage error	Operating cost ($)	Standard deviation	Operating cost
0	7467	0	7467
10	7568	15	7353
20	7636	25	7652
30	7695	30	7690

Table 7
Influence of uncertainty in renewable power generation.

Irradiance profile	PV_0	PV_f
Estimated operating cost ($)	7189	7417
Rescheduling/Regulation cost ($)	0	44.53
Actual rescheduled cost ($)	7189	7461.53

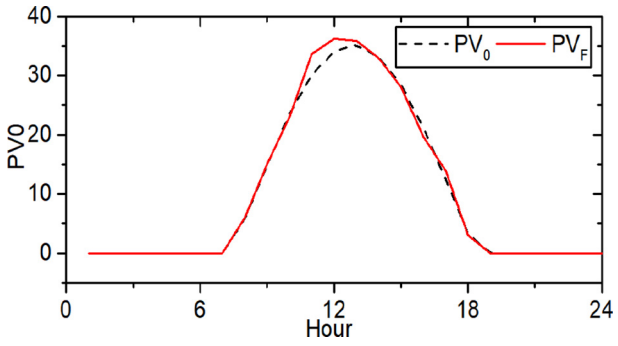

Fig. 8. Forecasted and actual values of solar power.

5. Conclusions

Geographic information system and weather parameter based DLR is proposed and its effectiveness in SCUCP is investigated. The results enable us to understand that the accuracy of DLR estimation increases when geographic information system is used along with weather variables. Also, wind speed and wind direction are found to have greater impact on DLR when compared to other variables. The proposed GISWDLR also results in lesser operating cost and enhanced security when compared to other methods. The enhanced operation of the proposed method is due to the following aspects.

1. Consideration of geographic parameters in DLR calculation.
2. Ability of BRPSO to handle the constraint more effectively compared to conventional enhanced priority list method.

The effective use of geographic information systems in estimation of DLR will improve cost economics and security of the power system in a smart grid environment. Hence, the proposed method will help generation and transmission companies in scheduling activities.

References

[1] M. Shahidehpour, H. Yamin, Z. Li, Market operations in electric power systems : forecasting, scheduling, and risk management, 2002. doi:10.1002/047122412X.
[2] M. Nick, O. Alizadeh-Mousavi, R. Cherkaoui, M. Paolone, Security constrained unit commitment with dynamic thermal line rating, (2015) 1–12.
[3] W. Winter, K. Elkington, G. Bareux, J. Kostevc, Pushing the limits: europe's new grid: innovative tools to combat transmission bottlenecks and reduced inertia, Power Energy Mag. IEEE 13 (2015) 60–74.
[4] P. Calistri, A. Conte, J.E. Freier, M.P. Ward, Geographic information systems: introduction, Vet. Ital 43 (2007) 379.
[5] V.C. Gungor, et al., A survey on smart grid potential applications and communication requirements, 9 (2013) 28–42.
[6] F. Yang, G. Liu, X. Chen, R. Lin, C. Xue, Power transmission lines maintenance system base on Google Earth (GE) platform, in: Annu. Rep. Conf. Electr. Insul. Dielectr. Phenomena, CEIDP, 2007: pp. 352–355.
[7] S. Amin, A. Ali-Eldin, H.A. Ali, A context-aware dispatcher for the internet of things: the case of electric power distribution systems, Comput. Electr. Eng. 52 (2016) 183–198.
[8] S. Uski-Joutsenvuo, R. Pasonen, Maximising power line transmission capability by employing dynamic line ratings–technical survey and applicability in Finland, Vtt.Fi. (n.d.). http://www.vtt.fi/inf/julkaisut/muut/2013/VTT-R-01604-13.pdf.
[9] C.J. Wallnerstrom, Y. Huang, L. Soder, Impact from dynamic line rating on wind power integration, Smart Grid, IEEE Trans. 6 (2015) 343–350.
[10] M. Askarpour, V. Zeinadini, Security-constrained unit commitment reaction to load and price forecasting errors, 2009 6th Int, Conf. Eur. Energy Mark. EEM 2009 (2009).
[11] D. Committee, I. Power, E. Society, IEEE standard for calculating the current-temperature relationship of bare overhead conductors, 2013.
[12] D. Douglass et al., Real-time overhead transmission line monitoring for dynamic rating, Power Deliv. IEEE Trans. (2014) 1.
[13] T. Krontiris, A. Wasserrab, G. Balzer, Weather-based Loading of Overhead Lines – Consideration of Conductor's Heat Capacity, in: Proc. Mod. Electr. Power Syst. 2010, 2010: pp. 1–8.
[14] J.F. Hall, A.K. Deb, Prediction of overhead transmission line ampacity by stochastic and deterministic models, IEEE Trans. Power Deliv. 3 (1988) 789–800.
[15] S.D. Foss, S.H. Lin, R.A. Maraio, H. Schrayshuen, Effect of variability in weather conditions on conductor temperature and the dynamic rating of transmission lines, IEEE Trans. Power Deliv. 3 (1988) 1832–1841.
[16] L. Ren, X. Jiang, G. Sheng, Research for dynamic increasing transmission capacity, Proc. 2008 Int. Conf. Cond. Monit. Diagnosis, C. 2008. (2007) 720–722.
[17] J.S. Engelhardt, S.P. Basu, Design, installation, and field experience with an overhead transmission dynamic line rating system, Proc. 1996 Transm. Distrib. Conf. Expo. (1996).
[18] M. Piekutowski, T.L. Le, M. Negnevitsky, Expert system application for the loading capability assessment of transmission lines, IEEE Trans. Power Syst. 10 (1995) 1805–1812.
[19] D.J. Morrow, J. Fu, S.M. Abdelkader, Experimentally validated partial least squares model for dynamic line rating, Renew. Power Gener. IET. 8 (2014) 260–268.
[20] J.L. Aznarte, N. Siebert, Dynamic line rating using numerical weather predictions and machine learning: a case study, IEEE Trans. Power Deliv. 32 (2017) 335–343.
[21] C. Black, W. Chisholm, Key considerations for the selection of dynamic thermal line rating systems, IEEE Trans. Power Deliv. 8977 (2014). 1 1.
[22] A. Michiorri, H.-M. Nguyen, S. Alessandrini, J.B. Bremnes, S. Dierer, E. Ferrero, et al., Forecasting for dynamic line rating, Renew. Sustain. Energy Rev. 52 (2015) 1713–1730.
[23] I. Albizu, E. Fernandez, A.J. Mazon, R. Alberdi, Forecast ratio and security analysis of rating forecasting methods in an overhead line, IET Gener. Transm. Distrib. 11 (2017) 1598–1604, https://doi.org/10.1049/iet-gtd.2016.1649.
[24] B. Banerjee, D. Jayaweera, S.M. Islam, Optimal scheduling with dynamic line ratings and intermittent wind power, PES Gen. Meet. | Conf. Expo. 2014 IEEE. (2014) 1–5.
[25] M. Nick, S.M. Ieee, O.A. Mousavi, R. Cherkaoui, S. Member, M. Paolone, et al., Integration of transmission lines dynamic thermal rating into real-time optimal dispatching of power systems, (2015) 0–5.
[26] V. Roberge, M. Tarbouchi, G. Labonte, Comparison of parallel genetic algorithm and particle swarm optimization for real-time UAV path planning, IEEE Trans. Ind. Informatics. 9 (2013) 132–141.
[27] V. Sharma, P.K. Singhal, R. Naresh, Binary fish swarm algorithm for profit-based unit commitment problem in competitive electricity market with ramp rate constraints, IET Gener. Transm. Distrib. 9 (2015) 1697–1707.
[28] M. Govardhan, R. Roy, Generation scheduling in smart grid environment using global best artificial bee colony algorithm, Int. J. Electr. Power Energy Syst. 64 (2015) 260–274, https://doi.org/10.1016/j.ijepes.2014.07.016.
[29] S. Dhanalakshmi, S. Baskar, S. Kannan, K. Mahadevan, Generation Scheduling problem by Intelligent Genetic Algorithm, Comput. Electr. Eng. 39 (2013) 79–88.
[30] B. Gjorgiev, D. Kančev, M. Čepin, A. Volkanovski, Multi-objective unit commitment with introduction of a methodology for probabilistic assessment of generating capacities availability, Eng. Appl. Artif. Intell. 37 (2015) 236–249.
[31] M. Neyestani, M.M. Farsangi, H. Nezamabadi-Pour, A modified particle swarm optimization for economic dispatch with non-smooth cost functions, Eng. Appl. Artif. Intell. 23 (2010) 1121–1126.
[32] K. Chandrasekaran, S.P. Simon, Binary/real coded particle swarm optimization for unit commitment problem, 2012 Int. Conf. Power, Signals, Control. Comput. (2012) 1–6.
[33] C.H. Ram Jethmalani, S.P. Simon, K. Sundareswaran, P. Srinivasa Rao Nayak, N. P. Padhy, Auxiliary hybrid PSO-BPNN based transmission system loss estimation in generation scheduling, IEEE Trans. Ind. Inf. 3203 (2016). 1–1.

[34] K.N.V.D. Sarath, V. Ravi, Association rule mining using binary particle swarm optimization, Eng. Appl. Artif. Intell. 26 (2013) 1832–1840.
[35] T. Niknam, M.R. Narimani, J. Aghaei, R. Azizipanah-Abarghooee, Improved particle swarm optimisation for multi-objective optimal power flow considering the cost, loss, emission and voltage stability index, IET Gener. Transm. Distrib. 6 (2012) 515.
[36] K. Chandrasekaran, S.P. Simon, Optimal deviation based firefly algorithm tuned fuzzy design for multi-objective UCP, IEEE Trans. Power Syst. 28 (2013) 460–471.
[37] R. Christie, Power systems test case archive, (2000). http://www.ee.washington.edu/research/pstca/.
[38] R.L. Cilibrasi, P.M.B. Vitányi, The Google similarity distance, IEEE Trans. Knowl. Data Eng. 19 (2007) 370–383.
[39] E. Delarue, D. Cattrysse, W. D'haeseleer, Enhanced priority list unit commitment method for power systems with a high share of renewables, Electr. Power Syst. Res. 105 (2013) 115–123.
[40] R. Dupin, A. Michiorri, Dynamic line rating forecasting, Elsevier Ltd, 2017. doi:10.1016/B978-0-08-100504-0.00013-5.
[41] V. Suresh, S. Sreejith, Economic dispatch and cost analysis on a power system network interconnected with solar farm, 5 (2015).
[42] S.P. Simon, N.P. Padhy, R.S. Anand, An ant colony system approach for unit commitment problem, Int. J. Electr. Power Energy Syst. 28 (2006) 315–323.
[43] L. Chen, J. Zhong, D. Gan, Optimal Automatic Generation Control (AGC) dispatching and its control performance analysis for the distribution systems with DGs, 2007 IEEE Power Eng. Soc. Gen. Meet. (2007) 1–6.